Measurements of the ion drift velocities in the presheaths of plasmas with multiple ion species

2013 JINST 8 C11020

(http://iopscience.iop.org/1748-0221/8/11/C11020)

J inst

PUBLISHED BY IOP PUBLISHING FOR SISSA MEDIALAB

RECEIVED: *September 14, 2013*
ACCEPTED: *October 3, 2013*
PUBLISHED: *November 21, 2013*

16th INTERNATIONAL SYMPOSIUM ON LASER-AIDED PLASMA DIAGNOSTICS,
22–26 SEPTEMBER 2013,
MADISON, WISCONSIN, U.S.A.

Measurements of the ion drift velocities in the presheaths of plasmas with multiple ion species

G. Severn,[a,1] C.-S. Yip[b] and N. Hershkowitz[b]

[a]*Department of Physics, University of San Diego,*
San Diego, California, 92110, U.S.A.
[b]*Department of Engineering Physics, University of Wisconsin-Madison,*
Madison, Wisconsin, 53706 U.S.A.

E-mail: severn@sandiego.edu

ABSTRACT: We have used a variety of diode lasers to perform laser-induced fluorescence (LIF) measurements that were the first to test the Bohm Criterion for multiple ion species plasmas. These measurements led to the discovery that a collective effect, ion-ion instability enhanced friction, is important for sheath formation in multiple ion species plasmas. New LIF schemes were pioneered in order to complete these experiments with diode lasers. With respect to a new LIF scheme for KrII, accessible to diode lasers, challenges remain fielding an ion flow diagnostic in low temperature plasmas.

KEYWORDS: Lasers; Plasma diagnostics - interferometry, spectroscopy and imaging

[1]Corresponding author.

doi:10.1088/1748-0221/8/11/C11020

Contents

1 **Introduction** 1

2 **Diode laser apparatus, and plasma discharge device** 3

3 **Comparison with the new theory** 6

4 **Development of a KrII ion flow diagnostic and the deconvolution problem** 8

5 **Summary** 11

1 Introduction

Plasma sheaths are characteristic of all bounded plasmas. They are electrostatic potential barriers that form to provide a balance of electron and ion fluxes to boundaries. The dynamic nature of their formation and existence was asserted by both Langmuir [1] and Bohm [2] each in their own way. The plasma sheath is critical to the operation of all devices which depend on plasmas. Examples range from light sources to material processing plasmas, to fusion plasmas as well as objects encountered in space physics. Langmuir and Bohm predicted that the ions in single ion species plasmas are supersonic at the sheath edge where their drift velocity is given by $v = c_s = \sqrt{T_e/m_i}$, where T_e is the electron temperature in eV and m_i is the ion mass. This requirement is now called the Bohm Criterion.

It is about 90 years since Langmuir defined the thin region of nonzero space charge interposed between the quasineutral bulk plasma and its boundary as the sheath, and it may seem odd that experiments that have tested theories of sheath formation have only recently been conducted. These experiments have waited on the development of a nonperturbing, spatially localized ion flow diagnostic, the tunable laser, to augment careful, and relatively nonperturbing, and spatially localized electrostatic potential measurements made by emissive probes. Such experiments were first conducted in mid 90's with dye lasers [3]. The advent of relatively inexpensive, and enormously less resource intensive tunable diode laser systems made such experiments more feasible. This paper discusses the first application of tunable diode laser systems to the problem of sheath formation in more general plasmas than the single ion species plasmas treated by Langmuir and Bohm, (indeed, these were the first experiments to treat the problem of sheath formation in multiple ion species plasmas experimentally, of any kind) and gives an overview on the status of our experiments, including recent work with a KrII ion flow diagnostic for low temperature plasmas.

These experiments have driven diagnostic development in the field of diode laser-based laser-induced fluorescence (dLIF). The motivation was the desire to understand sheath formation in complex, general plasmas. The Bohm Criterion has been generalized [4, 5] for the case of multiple positive ion species plasma to give a condition $1 \geq \sum_i (n_{io} c_j^2)/(n_{eo} v_{io}^2)$, when the ion temperature

2013 JINST 8 C11020

$T_i \ll T_e$, as is the case in low temperature plasmas. The subscript o refers to the speeds at the sheath edge. This is one condition with as many variables as the number of ion species. For the case of two ions, this condition admits a continuum of solutions in which either ion may have an arbitrarily large speed at the sheath edge. However, it was generally believed that sheath formation would proceed in pretty much the same fashion as in single species plasmas, and that individual ion species would reach the sheath edge at their own individual Bohm speeds. There were a number of theoretical works [6, 7] that indicated that the Bohm Criterion held strictly only for collisionless plasmas, and was an approximation that grew poorer and poorer with finite collisionality. This is one of the immediately obvious simple solutions to the generalized Bohm criterion. Given the growing importance of plasma science and technology at the turn of the new millenium, it seem critical to us to put these basic ideas of plasma physics to the test.

As mentioned above, the generalized Bohm Criterion is no longer determinate. Beside the simple solution that all ion species reach their individual Bohm speeds at the sheath edge, there is is another simple solution, namely that all ions reach the same speed at the sheath edge, that is, at the system sound velocity $c_s = (\sum_i [c_{s,1}^2 \{n_{io}/n_{eo}\}])^{1/2}$. Our experiments in weakly collisional, weakly ionized plasmas containing two positive ion species with comparable ion concentrations have found conclusively [12–14] that the generalized Bohm Criterion is satisfied, with a solution very close to the second simple solution.

The problem of course was that at the time we discovered this, there was no theoretical basis for preferring this solution to one in which all classes reached their own Bohm speeds at the sheath edge. Beyond, however, ion neutral collisions, the process of sheath formation in two species plasmas involves streaming ions with different flow velocities. It was quite plausible to ignore friction arising from ion-ion Coulomb collisions since their characteristic scale lengths were much, much longer than ion-neutral collision scale lengths in weakly ionized plasmas. Recently, Baalrud [10, 11] et al. theoretically determined the solution to the Bohm Criterion in a multispecies plasma by including the effects associated with the presence of instability enhanced collisional friction between the ion species. In their prediction, the difference between the drift velocities of the ion species at the sheath edge was small but nonzero, and depended on the difference in ion concentrations. They showed that when the ion concentrations are comparable in a two ion species plasma, each ion species reaches the sheath edge at nearly the system sound speed. They also predicted that the small difference in drift velocity between the two species is insensitive to relative ion concentrations for n_{Ar}/n_e between 0.2 and 0.7. When one ion species dominates, each ion species is predicted to reach the sheath edge at its own Bohm velocity. We reported the first experimental test of this model [14].

Baalrud et al. calculated the enhancement of the collisional friction associated with the ion-ion instability, and incorporated that into the ion momentum equation. They found that the collisional friction would bring the two species' drift velocities closer together until the velocity difference reached a critical velocity given by

$$\Delta V_c = V_2 - V_1 = \sqrt{\frac{1+\alpha}{2\alpha}} \sqrt{v_{T1}^2 + \alpha v_{T2}^2}, \tag{1.1}$$

where $\alpha = n_1 M_2/(n_2 M_1)$. Note that in the limit that $T_i/T_e \to 0$ both species are lost at the system sound velocity. The theory made several approximations the most important of which was using the fluid approximation for ΔV_c.

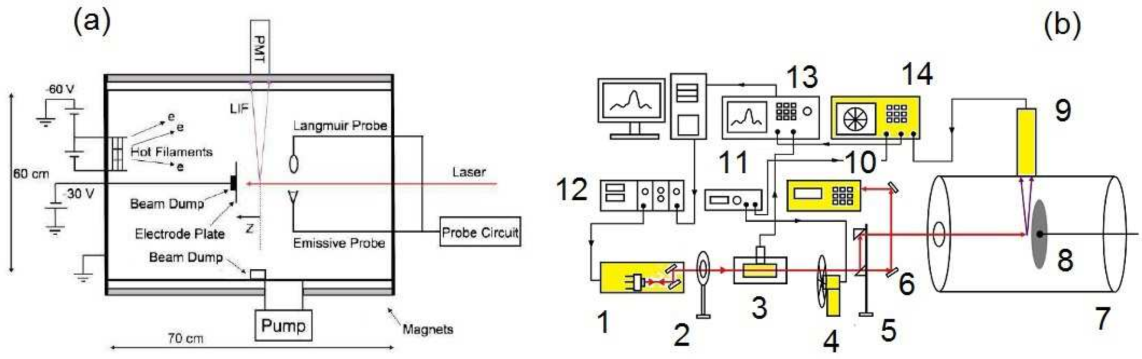

Figure 1. (a) Schematic diagram of the typical experimental setup. (b) Schematic diagram of the LIF experiment: (1) laser head (2) iris, (3) iodine cell, (4) mechanical chopper, (5) periscope, (6) mirrors, (7) chamber, (8) electrode plate and beam dump, (9) photomultiplier tube, (10) wavemeter, (11) chopper controller, (12) laser driver, (13) oscilloscope and (14) lock-in amplifier. The arrows indicate the direction of the signal flow.

2 Diode laser apparatus, and plasma discharge device

The experiments were carried out in a multidipole confinement device shown schematically in figure 1 (a). and is described in detail elsewhere [14]. The base vacuum for most measurements was approximately between 0.3–1.0 μTorr. Permanent magnet rows (peak fields, 0.1 T) with alternating magnetic polarities, were mounted axially, but not on the chamber end walls. Plasma was produced by electron emission from 21 hot thoriated tungsten filaments (0.1 mm in diameter, approximately 10 cm long) biased at -60 V with respect to the grounded chamber. A stainless steel plate of radius 7.5 cm was located along the axis of the chamber biased at -50 V. A 0.75 cm radius hole backed by a razor blade stack used as a laser beam dump was located in the center of the plate. The plate was displaced in a direction parallel to the incident laser beam to measure the ion velocity as a function of position from the plate, while the collection optics and the photomultiplier tube (PMT) remained fixed. In addition, a 8 cm$\times$12 cm razor blade stack anti-reflector was placed on the axis of signal collection of the PMT to reduce stray light reflection off the chamber wall.

The LIF technique, is described in detail in many places [8], although its inclusion as a standard diagnostic for ion dynamics in plasmas date back to Stern's pioneering efforts [9]. In noble gas discharges, one selects a metastable ion state known to be sufficiently populated in a plasma discharge, directs a tunable laser light source through the plasma so as to intersect a region in the plasma to be diagnosed with the optical axis of a train of collection optics terminated by a fluorescence collection detector, often a photomultiplier tube (PMT). A narrowband interference filter whose center wavelength matches the wavelength of the fluorescence transition reduces stray light. Further details concerning noise-to-signal reduction using the lock-in technique we employed are quite standard and are also described in detail elsewhere [14]. Our installation of LIF related instruments on our optics table is indicated in figure 1 (b).The wavelength of the laser itself is chosen to match the energy gap between the metastable state and an excited state possessing one dominant decay (fluorescent) transition, which, preferably is at the blue end of the visible spectrum (to match the peak sensitivity of many PMT's). These 3 energy levels are commonly referred to as an "LIF

Table 1. Summary of LIF schemes in ArII accessible by available diode lasers, c.1995–2000. For comparison, the standard scheme used by dye lasers is included. This list of course is not exhaustive; only the schemes with the highest transition probabilities from the excited states have been included. The metastable state is state 1 in the 3 level LIF scheme. The fluorescence transition connects the excited state (state 2) with the state to which it decays (state 3). The absolute spontaneous transmission probabilities(A_{12}, A_{23}) and the branching ratio (β_{23}) for the fluorescence transition are also given. The last column gives the minimun velocity resolution (Δv) of that scheme. All wavelengths are given for vacuum conditions.

Scheme no.	Metastable state	Fluorescence transition	λ_{12} (nm)	λ_{23} (nm)	A_{12} (10^8 s^{-1})	A_{23} (10^8 s^{-1})	β_{23}	Δv (m/s)
1	$3d'\,^2G_{9/2}$	$4p'\,^2F^o_{7/2}$- $4s'\,^2D_{5/2}$	611.66	461.08	0.200	0.789	0.665	12.2
2	$3d\,^4F_{7/2}$	$4p\,^4D^o_{5/2}$-$4s\,^4P_{3/2}$	668.61	442.72	0.107	0.817	0.616	7.2
3	$3d\,^4F_{9/2}$	$4p\,^4D^o_{7/2}$-$4s\,^4P_{5/2}$	664.55	434.93	0.147	1.171	0.810	9.8
4	$3d\,^4F_{7/2}$	$4p\,^4D^o_{7/2}$-$4s\,^4P_{5/2}$	688.85	434.93	0.009	1.171	0.810	0.6

scheme”. The scheme in common use for argon discharge plasmas at the time these experiments commenced required an excitation wavelength of 611 nm, much shorter than any commercially available diode laser at the time. The industry standard red diode laser then was near 670 nm. Still, it was decided that the experiments were to be done with diode lasers rather than dye lasers because of the almost order of magnitude in cost savings, and the dramatically reduced power and water recourses required.

Finding an LIF scheme suitable for diode lasers in Ar discharges was pioneered by one of us in collaboration with Edrich and McWilliams [15]. We simply studied the energy levels of ArII and found the metastable states following the rules of LS coupling, and looked for excited states that allowed for transitions accessible then to visible diode lasers. These are shown in table 1. It is very difficult to predict the population of a metastable state in a given plasma discharge. McWilliams graciously put at our disposal a dye laser and the dye DCM [16] and we simply explored for the sought after schemes. We found those LIF schemes listed in the table, although we note that the population of the $^4F_{9/2,7/2}$ metastables was found to be an order of magnitude diminished relative the $3d'\,^2G_{9/2}$ metastable excited by the dye laser tuned to 611 nm. Moreover, in the Irvine Plasma Torus [17], (typical plasma parameters were: plasma density,$n_e < 10^{11}$ cm^3, electron and ion temperatures, $T_e < 5$ eV, $0.1 < T_i < 2$ eV) it was found that the minimum laser power sufficient to produce a useful LIF was 15 mW, considerably in excess of the few mW available in solitary diode laser systems in either Littrow or Littman-Metcalf optical cavities, the so-called extended cavity diode laser systems (ecdl). We used a spatially mode matched tandem system comprising a tapered chip amplfier locked to an ecdl laser system, the so-called Master Oscillator Power Amplifier (MOPA) system. Our system furnished up to 500 mW of power. It was with this system that we began our work measuring ion velocity distribution functions (ivdfs) in multiple ion species plasmas in argon discharges in which Xe gas was added.

Eventually it became necessary to employ separate lasers to measure ivdfs for ArII and XeII ions, without the aid of dye lasers (again for reasons of cost savings and so forth). Again, the typical transition employed for use with dye lasers, at 605 nm [18] was not accessible to available diode lasers, so we again developed a novel LIF scheme [19] suitable for visible (available) diode lasers.

2013 JINST 8 C11020

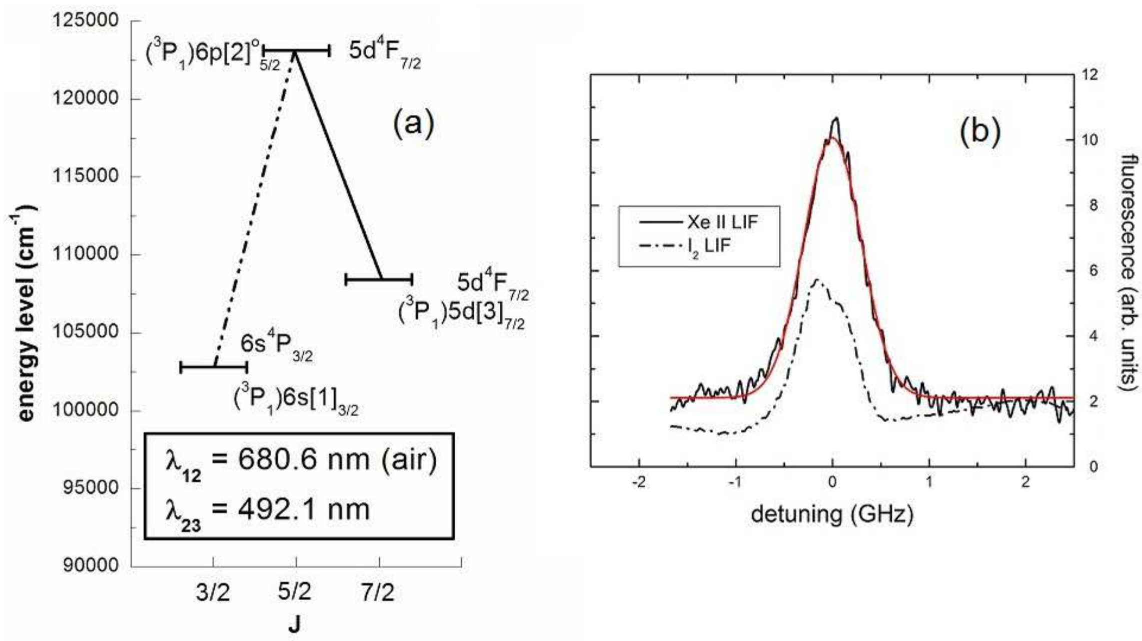

Figure 2. LIF scheme for XeII accessible by visible diode lasers near 680 nm.

This proved to be a thornier problem than was the case for diode laser based LIF (dLIF) for ArII. The LIF scheme we settled on is shown in figure 2 (a), and it was found in much the same way, and it was found simply by studying XeII energy levels in the literature. We estimated that at a wavelength of 680.574 nm we could excite metastable Xe+ in the metastable state, $5p^4(^3P_1)5d[3]_{7/2}$, to the $5p^4(^3P_1)6p[2]^o_{5/2}$ state. The fluorescence transition would then be to the $5p^4(^3P_1)6s[1]_{3/2}$ state, producing a detected photon at 492.15 nm (air wavelengths).

Once one has a scheme to test, one then looks to see if the line has been seen in the literature (if one does not have the luxury of searching for the line directly in ones plasma discharge with a suitable light source). We did find references [21] (fast ion beam laser spectroscopy, FIBLAS) to a transition from the putative metastable state to an excited state at a wavelength near and industry standard red wavelength, 680.574 nm, although the coupling schemes used for identifying the spectroscopic terms were found not be uniform, hence the two different nomenclatures (jK and LS coupling) shown in figure 3. It was found that there was a disagreement in the literature between measured excited state lifetimes which exceeded experimental error. Finally a re-evaluation of the entire energy level structure of XeII was performed and published [22]. It was found that *jK* coupling is superior (the eigenstates, purer) to the old *LS* coupling analysis, and that many excited state misidentifications could be resolved. The resolution of misidentified states attaching to our LIF scheme is described elsewhere [19]; we only want to point out that detecting fluorescence in a FIBLAS experiment is no proxy for obtaining useful LIF signals in any particular plasma discharge. We simply bought an appropriate diode laser and hoped for the best. Of course it was an extreme relief to acquire a good LIF signal (figure 2 (b)).

Two more aspects of the over all dLIF process are worthy of note. Diode laser technology evolves at a pace consistent with its own economic drivers (among which are *not* the needs of the spectroscopy community). By the later part of the 2000's, the output power of ecdl lasers in Littrow configurations had improved considerably, achieving output powers in excess of 20 mW. Scime et al. [20] had pioneered their use. The footprint of the laser on the optics table had shrunk by roughly a factor of 100. Secondly, Scime had also convinced us to use wavelength meters for coarse wavelength tuning. Our absolute wavelength calibration employed an iodine gas cell along with an atlas of verified absorption lines [23]. For coarse tuning, the Burleigh WA-1000 wavemeter proved invaluable. However, we found that simply repositioning the wavemeter on the optics table occasioned very slight displacements of measured wavelengths (not to mention shipping the wavemeter between labs) of order of 1 GHz, a trivially small amount except in comparison with the FWHM of an ivdf in a low temperature plasma, a difference that could make a radical difference in determining the fiducial line center for Doppler shift assessments of ion velocity. Wavemeters are vital, but so are molecular absolute wavelength calibrations. We calibrated our wavelengths against measure fluorescence from our iodine cell and the measured iodine atlas's of Salami and Ross [24] and Gerstenkorn and Luc [23], and found that there was a + 1.68 GHz shift between our measured frequencies and those of Salami and Ross.

Finally, we mention briefly that the ion velocity distribution functions and their moments were obtained from the LIF signals as follows. The IVDF, $f(v_z,z)$, was obtained from the LIF signal, $f(\Delta f_d,z)$, a function of the detuning frequency, using the first order Doppler shift,

$$v_z = \frac{c\Delta f_d}{f_o + \Delta f_d} \approx \frac{c\Delta f_d}{f_o} = \lambda_o \Delta f_d, \tag{2.1}$$

where v_z is the ion velocity, c is the speed of light, λ_o is the excitation wavelength at the line center, f_o is the excitation frequency at the line center, Δf_d is the detuning from the line center. The n_{th} moment of the IVDF,

$$\langle v_z \rangle^n = \int_{-\infty}^{\infty} (v_z)^n f(v_z,z) dv_z / \int_{-\infty}^{\infty} f(v_z,z) dv_z. \tag{2.2}$$

was used to compare with theory. It was assumed that the ion metastable state is in thermal equilibrium with the ground state ion.

3 Comparison with the new theory

The first LIF measurements in a two-ion species plasma were performed on ArII ions in an Ar+He plasma ($P_{ArI} \sim 0.1\,\mathrm{mTorr}$, $0 \leq P_{He}/P_{Ar} \leq 25$, and $0 \leq n_{He^+}/n_e \leq 0.5$, $T_e \leq 2\,\mathrm{eV}$), and were reported by Severn et al. [25] The results were surprising and unexpected. LIF measurements clearly showed that the rms speed of the ArII ions exceeded their own Bohm speed. The measurement technique was directly compared with that in pure Ar plasma to see if the simple Bohm Criterion was satisfied at the sheath edge, and it was, within experimental error.

The rms speed (requiring an estimate of the 2nd moment of the ivdf) was compared with theory since in Bohm's original work, the criterion was based on a minimum kinetic energy condition required of ions for the sheath to form, rather than a flow condition. A family of measured ivdfs is shown in figure 3 (a), and the rms speed as a function of position relative to the boundary plate (along with an electrostatic potential profile measured with an emissive probe) is shown in figure 3 (b). It was hard to escape the conclusion that ArII ions fall into the sheath moving

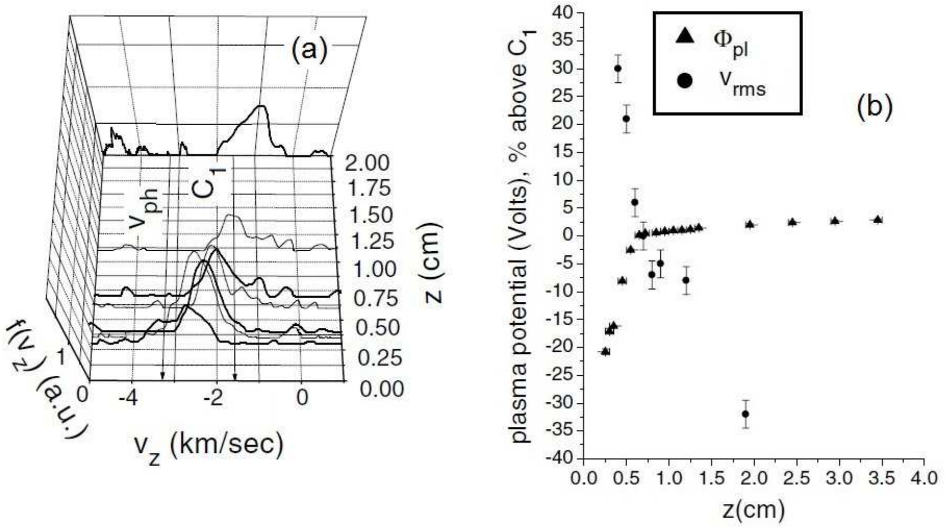

Figure 3. (a) A family of ivdfs for the two ion plasma (Ar + He). The ion acoustic speed of the two ion plasma in the bulk plasma is given by v_{ph}. (b) The plasma potential profile for Ar + He plasmas reveals that the rms velocity of the ArII ions is well beyond the individual Bohm speed, c_1, and approaching the ion sound speed of the system (as measured in the bulk) at the sheath edge.

significantly faster in the Ar-He plasma than they do in the pure Ar plasma, by more than 75% faster, indeed, reaching the ion sound speed of the bulk plasma (within error). We note that in these experiments the ratio of the densities of the two ions was close to unity.

Since we had no LIF scheme for HeII (it is still the case that there is no viable LIF scheme for HeII suitable for diode lasers), we could not be sure whether the generalized Bohm Criterion was satisfied, and if, as a result whether the He ions were reaching the sheath edge at a speed much reduced compared with their individual Bohm velocity. It occurred to us to the try Ar + Xe mixtures to see if ArII ions would behave in those plasmas as we surmised was the case for HeII in Ar+He plasma. We also aimed at finding a new LIF scheme for XeII as described previously in order to test the generalized Bohm Criterion. In a series of experiments reported by Lee [12, 13], it was confirmed that ArII ions reach the sheath edge at speeds much reduced relative to their individual Bohm speed, and once we were able to perform XeII LIF measurements, we verified that in a two-ion species plasmas of small but finite collisionality, the generalized Bohm Criterion was satisfied, within experimental error, in the equality at the sheath edge. We verified that when the concentration ratio is close to unity, both ion species fell into the sheath at speeds very nearly equal to the ion sound speed of the bulk plasma. A family of XeII ivdfs is shown in figure 4 (a), and an axial profile of speed of both ions (along with the electrostatic potential profile measurement, locating the sheath edge) is shown in figure 4 (b).

At this point, we recognized that something was wrong. There seemed to be a kind of flow locking mechanism that kept the ion flows at comparable speeds all along the presheath, one which could not be accounted for by ion neutral collisions, as none of the resonant or non-resonant charge exchange collision lengths were equivalent. Not long after this, a new theory of sheath formation which treated ion-ion flow instabilities arose. Along with his collaborators, a former student from

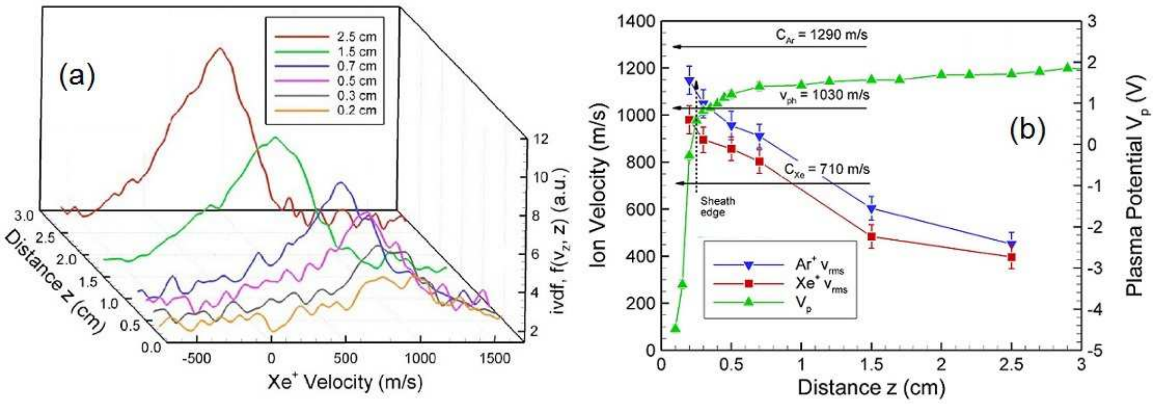

Figure 4. (a) Xe IVDFs as a function of distance z from the plate in the Ar 0.5+Xe 0.2 mTorr plasma. (b) Spatial profiles of the plasma potential and Ar+Xe velocities in the Ar 0.5+Xe 0.2 mTorr plasma.

our group, Baalrud et al. [10, 11] was able to show theoretically that the ion-ion flow instability significantly enhanced the effective Coulomb friction between the two flowing species, providing for an interaction between the ion classes that effectively slowed the one and accelerated the other, a collective effect that we had seen in the experimental results.

A series of experiments reported on by Yip et al. [14, 26] then focused on a comparison of the experimental measured drift velocities for argon and xenon ions versus relative argon ion concentration with theory curves based on the predictions of Baalrud at el. The data displayed are moment calculations of ivdfs with the observed xenon ion temperature of approximately 0.05 eV and argon ion temperature of approximately 0.043 eV. The dashed theory curve gives results in which a fluid theory was used to express the dispersion relation for the instability while the solid curve represents the use of the same dispersion relation corrected for finite ion thermal effects. The revised version of the theory assumed that the ivdfs were Maxwellian, and predicted that the magnitude of the ion drift velocity differences were given by

$$\Delta V_c = -\frac{3}{2}|v_{T2} - v_{T1}| + \sqrt{\frac{1}{2}\left(v_{T1}^2 + v_{T2}^2 + \frac{n_2 T_1}{n_1 T_2} v_{T1}^2 + \frac{n_1 T_2}{n_2 T_1} v_{T2}^2\right)}. \tag{3.1}$$

It was apparent that the observed drift velocities and the prediction were in excellent agreement. This provided strong support for the argument that instability-enhanced collisional friction between ion species in the presheath of weakly collisional plasma with two ion species causes both ion species to be lost at close to the system sound velocity over a wide range of relative concentrations (see figure 5). It also shows that when the concentration ratios are very large, each species is lost at close to its own individual Bohm velocity, which was itself a new experimental result.

4 Development of a KrII ion flow diagnostic and the deconvolution problem

We sought to test a new ion for analysis, KrII, in order to try the 3 ion problem of sheath formation [27] and we chose to test a new LIF scheme requiring excitation near 729 nm, which at the

2013 JINST 8 C11020

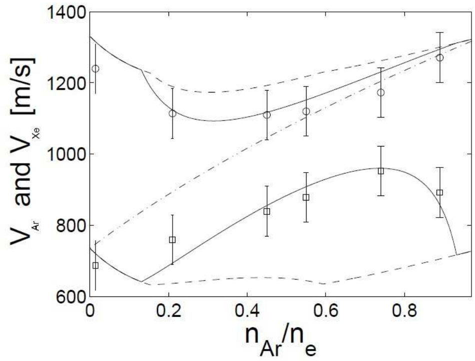

Figure 5. Comparison of data and the prediction of the revised theory. The circles are the measured argon drift velocity and the squares are the measured xenon drift velocity. The dashed line uses the fluid plasma dispersion relation for the two stream instability, while the solid line is the new prediction which incorporates finite ion thermal corrections to the dispersion relation. The system ion acoustic velocity is represented by the dashed dotted line.

time of our proposal in 2009 had not, to our knowledge, been successfully subjected to LIF analysis in low temperature plasmas using diode lasers. Krypton had been a focus of attention in the Hall Thruster community as a reasonable propellant to substitute for xenon, which is much more expensive. Recently, some excellent work done with diode laser based KrII LIF measurement acquired in the plume of a 200 W laboratory BHT-200-X3 Hall effect thruster has been published by Hargus et al. [28] using the LIF scheme that we had proposed, exciting from the metastable state $4p^4 4d^4 D_{7/2} \rightarrow 4d^4 5p^4 P^0_{5/2} \rightarrow 4d^4 4d^4 P_{5/2}$, with an excitation wavelength of 728.98 nm (air), and with a fluorescence wavelength of 473.90 nm. The unfolding of the ivdf from the LIF signal is complicated by the presence of isotope shifts, along with the hyperfine splitting of an odd A isotope ($^{83}Kr_{36}$). Only 6 of the known isotopes are of significant fractional importance in naturally occurring krypton, as shown in figure 6 (a). The problem then is one of deconvolution, where one aims at finding the frequency space line spreading function (the ivdf) that attaches to the line spectrum (which the isotopes compose) from the measured LIF signal. The quantum physics of the energy levels involved in the excitation transition is well described in Hargus, et al. [28]. A key feature in the deconvolution process is the ratio of the thermal Doppler broadening and to the isotope shifts between the central most prevalent isotope ($^{84}Kr_{36}$) and its satellite lines. The isotope shifts (in this case, roughly 0.4 GHz on either side of the main peak) set an ion temperature above which deconvolution algorithms tend to work smoothly. The Hall Thruster plasma ion temperature was found to be in excess of 5000 K (corresponding to a FWHM Doppler broadening of 2.3 GHz) and they reported that there was no essential difference between the LIF signal and the deconvolved ivdf.

In our case, the ions are typically an order of magnitude cooler, which makes the deconvolution much more difficult. We measured the LIF signal in the bulk plasma in a Kr discharge plasma, with neutral pressure of 0.56 mTorr, an electron temperature and density of 2.8 ± 0.1 eV, and 3.3×10^{10} cm^{-3}, respectively. The FWHM of the LIF signal (1.1 GHz) corresponded to an ion temperature of about 1,100 K, much hotter than is typical for ions in such discharge devices, and so we had clearly seen the effects of the thermalized isotope shift contributions. By simply

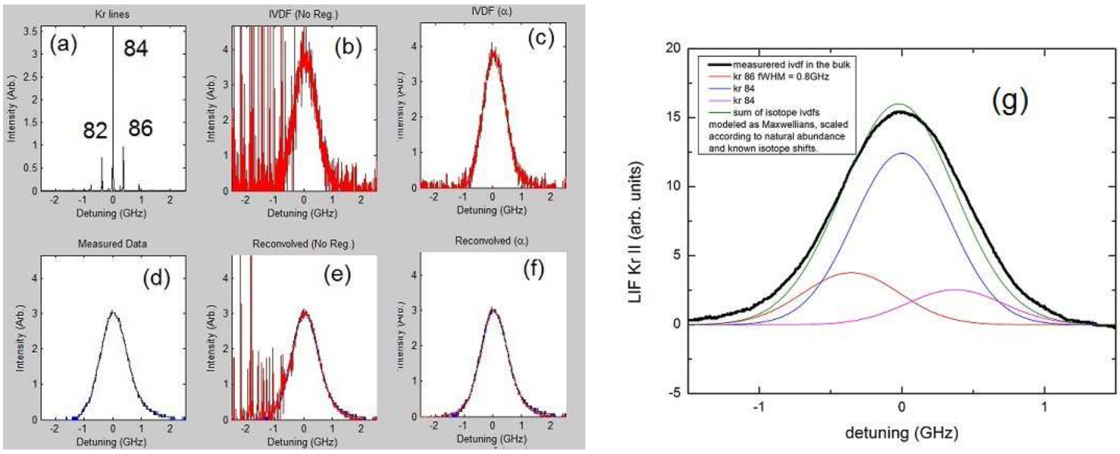

Figure 6. Kr II LIF signal in the bulk plasma consistent with an ion temperature of 1,100 K, Doppler broadened FWHM 1.1 GHz, modeled by the simple sum of 3 Maxwellians with FWHM's of 0.8 GHz, or 580 K.

fitting Gaussians for the central 3 most prominent isotopes (which account for 85% of a naturally occurring Kr) we were able to approximately fit the measured LIF signal, as shown in figure 6 (g).

But fitting Gaussians cannot help unfolding of very asymmetric ivdfs we expect to find near the sheath edge. The LIF signal convolves isotope shifts, thermal spreading, and and secular drift due to fluid flow, and each of these effects are of the same order of magnitude. The ion drift velocities are expected to be the order of the ion sound speed, which for electron temperatures typical of thermionic discharges in multidipole confinement devices yields for KrII a speed of nominally 1km/s and a Doppler shift of nominally 1 GHz. At the sheath edge we expect therefore that the details of the shape of an asymmetric ivdf distended on the low velocity side by charge-exchange collisions, convolved with isotopes shifted from each other by gaps of nearly the same order of magnitude, and along with a thermal spread also of the nearly the same order of magnitude may get lost in an LIF signal that will not look like the underlying ivdf.

What we have accomplished so far is the implementation of a noise tolerant deconvolution algorithm, Tikhonov Regularization [29], following the work of Hargus et al., with a focus on the signal we've measured in the bulk plasma far from the sheath edge. Our results are shown in fig 6 (b)–(f). The panel (a) shows the input isotope line spectra, and the measured LIF signal (d). Panels (b) and (c) show the deconvolved ivdf both with and without Tikhonov regularization. Panels (e) and (f) show the reconvolved signals (the ivdf convolved with the line spectrum matrix, to be described presently) compared with the measured LIF signal, indicating the effect of (amelioration of) noise. Briefly, Tikhonov Regularization is a procedure for making a digital deconvolution more robust with respect to the presence of noise. One wants to recover by deconvolution a line broadening shape, that is, the ion velocity distribution function, designated as the digital array $\mathbf{x}$, from a digitally measured LIF signal, designated as the array $\mathbf{b}$, where one models the signal measured as a convolution (operator A) of the isotope spectra and the ivdf, $A\mathbf{x} = \mathbf{b}$, where, A is an $n \times n$ matrix, and where x and b are column vectors with n elements. Deconvolution is 'simply' $\mathbf{x} = A^{-1}\mathbf{b}$.

The convolution operator, row by row, is essentially a shifted record of the isotope spectra. The problem of course is that many of the eigenvalues of the matrix A are inevitably small and are made less well known by noise (in the measured signal), which makes A almost uninvertible. One ameliorates their effect through a singular value decomposition of A, $\mathbf{A} = U\Sigma V^*$, where U and V are unitary matrices, and then one attempts to filter out contributions of the tiniest ith singular value of the matrix Σ using a *filter factor*, f_i with a 'regularization parameter' , α, $f_i = \sigma_i^2/(\sigma_i^2 + \alpha^2)$, yielding a modified matrix, Ψ, and giving an approximation of the desired inverted matrix, $A^{-1} = V\Psi^{-1}U^*$ that minimizes $A\mathbf{x} - \mathbf{b}$ element by element. In the bulk plasma our deconvolved ivdf is in good agreement with the Maxwellian fit, but with the possibility of deconvolving arbitrary ivdf's at the sheath edge. The problem of course is that technique is not up to recovering truly arbitrary functions. We also have seen the deconvolved ivdf's in the bulk look essentially the same as the LIF signal, although we don't expect this to be the case at the sheath edge. This is the challenge that remains in making the technique really work.

5 Summary

The dLIF measurements described here were the first measurements of any kind to test the Bohm Criterion for multiple ion species plasmas. They led to the discovery that a collective effect (ion-ion instability enhanced friction) is important for sheath formation in multiple ion species plasmas, and this in turn has lead to a new way of thinking about sheath formation. Further, dLIF measurements have for a long time been useful for measuring fluid-theoretic quantities, and these measurements are among those that have played a role in verifying quantities of direct importance in kinetic theory. At every step in this particular avenue of research, we had to develop new LIF schemes suitable for diode lasers in order to accomplish the measurements, and in particular, the KrII ivdfs are among the first measured in relatively low temperature plasmas. The problem of realizing a KrII ion flow diagnostic in low temperature plasmas near plasma boundaries is still in process.

Acknowledgments

This work was supported by U.S. Department of Energy Grant No. DE-FG02-97ER54437, No. DE-SC0001939 and No. DE FG02-03ER54728, National Science Foundation Grants No. CBET-0903832, and No. CBET-0903783, and No. PHYS-1206421. One of us (G.D.S.) would like to thank our visiting High School student, Ms. Jenny Collins, for fabricating a Langmuir Probe and interpreting its results, and USD undergraduate, Mr. Christopher Yip, for implementing Tikhonov Regularization in Matlab®.

References

[1] L. Tonks and I. Langmuir, *A General Theory of the Plasma of an Arc* *Phys. Rev.* **34** (1929) 876; I. Langmuir, *Electric discharges in gases at low pressures*, *J. Franklin Inst.* **214** (1932) 275.

[2] D. Bohm, *The characteristics of electrical discharges in magnetic fields*, chapter 3, McGraw-Hill, New York, U.S.A. (1949).

[3] M. Goeckner, J. Goree and T. Sheridan, *Laser-induced fluorescence characterization of a multidipole filament plasma*, *Phys. Fluids* **B 3** (1991) 2913.

[4] K.-U. Riemann, *The Bohm criterion and boundary conditions for a multicomponent system*, *IEEE T. Plasma Sci.* **23** (1995) 709.

[5] R.N. Franklin, *Plasmas with more than one species of positive ion and the Bohm Criterion*, *J. Phys.* **D 33** (2000) 3186.

[6] R.N. Franklin and J. Snell, *The plasma-sheath transition with a constant mean free path model and the applicability of the Bohm criterion*, *Phys. Plasmas* **8** (2001) 643.

[7] H.-B. Valentini, *Bohm criterion for the collisional sheath*, *Phys. Plasmas* **3** (1996) 1459.

[8] D. Hill, S. Fornaca and M.Wickham, *Single frequency scanning laser as a plasma diagnostic*, *Rev. Sci. Instrum.* **54** (1983) 309.

[9] R. Stern and J. Johnson, *Plasma Ion Diagnostics Using Resonant Fluorescence*, *Phys. Rev. Lett.* **34** (1975) 1548.

[10] S. Baalrud, J. Callen and C. Hegna, *Instability-Enhanced Collisional Friction Can Determine the Bohm Criterion in Multiple-Ion-Species Plasmas*, *Phys. Rev. Lett.* bf 103 (2009) 205002.

[11] S. Baalrud and C. Hegna, *Determining the Bohm criterion in plasmas with two ion species*, *Phys. Plasmas* **18** (2011) 023505.

[12] D. Lee, L. Oksuz, N. Hershkowitz and G. Severn, *Laser-induced fluorescence measurements of argon ion velocities near the sheath boundary of an argon-xenon plasma*, *J. Phys. D* **39** (2006) 5230.

[13] D. Lee, N. Hershkowitz and G. Severn, *Measurements of* Ar^+ *and* Xe^+ *velocities near the sheath boundary of Ar-Xe plasma using two diode lasers*, *Appl. Phys. Lett.* **91** (2007) 041505.

[14] C.-S. Yip, N. Hershkowitz and G.D. Severn, *Experimental Test of Instability-Enhanced Collisional Friction for Determining Ion Loss in Two Ion Species Plasmas*, *Phys. Rev. Lett.* **104** (2010) 225003.

[15] G.D. Severn, D.A. Edrich and R. McWilliams, *Argon ion laser-induced fluorescence with diode lasers*, *Rev. Sci. Instrum.* **69** (1998) 10.

[16] U. Brackmann, *Laser Dyes*, Lambda Physik, Göttingen, Germany (1997), and references therein.

[17] R. McWilliams and R. Platt, *Fast-wave current drive in the Irvine torus*, *Phys. Rev. Lett.* **56** (1986) 835.

[18] R.J. Cedolin, W.A. Hargus Jr., P.V. Storm, R.K. Hanson and M.A. Cappelli, *Laser-induced fluorescence study of a xenon Hall thruster*, *Appl. Phys.* **B 65** (1997) 459.

[19] G. Severn, L. Dongsoo and N. Hershkowitz, *Xenon ion laser-induced fluorescence using a visible tunable diode laser near 680 nm*, *Rev. Sci. Instrum.* **78** (2007) 116105.

[20] A.M. Keesee, R. Boivin and E.E. Scime, *Laser-induced fluorescence measurements of three plasma species with a tunable diode laser* , *Rev. Sci. Instrum.* **75** (2004) 4091.

[21] L. Broström, S. Mannervik, A. Passian and G. Sundström, *Investigation of some transitions and lifetimes in Xe II*, *Phys. Rev.* **A** bf 49 (1994) 3333, see figure 4, in particular.

[22] J.E. Hansen and W. Persson, *Revised analysis of singly ionized xenon, Xe II*, *Phys. Scr.* **36** (1987) 602.

[23] S. Gerstenkorn and P. Luc, *Atlas du Spectre d'Absorption de la Molecule d'Iode. Vol. II.*, Laboratoire Aime Cotton, CNRS II, Orsay, France (1993).

[24] H. Salami and A.J. Ross, *A molecular iodine atlas in ascii format*, *J. Mol. Spectrosc.* **233** (2005) 157.

[25] G.D. Severn, X. Wang, E. Ko and N. Hershkowitz, *Experimental Studies of the Bohm Criterion in a Two-Ion-Species Plasma Using Laser-Induced Fluorescence*, *Phys. Rev. Lett.* **90** (2003) 145001.

2013 JINST 8 C11020

[26] N. Hershkowitz, C.-S. Yip, and G.D. Severn, *Experimental test of instability enhanced collisional friction for determining ion loss in two ion species plasmas*, *Phys. Plasmas* **18** (2011) 057102.

[27] P.W. Anderson, *More Is Different*, *Science* **177** (1972) 393.

[28] W.A. Hargus Jr., G.M. Azarnia, and M.R. Nakles, *Kr II laser-induced fluorescence for measuring plasma acceleration* *Rev. Sci. Instrum.* **83** (2012) 103111.

[29] M. Fuhry and L. Reichel, *An algorithm for second order initial and boundary value problems with an automatic error estimate based on a third derivative method*, *Numer. Algorithms* **59** (2012) 433.

2013 JINST 8 C11020